Polyelectrolyte-Induced Reduction of Exfoliated Graphite Oxide: A Facile Route to Synthesis of Soluble Graphene Nanosheets

Sheng Zhang,[†,‡,§] Yuyan Shao,[‡,§] Honggang Liao,[‡] Mark H. Engelhard,[‡] Geping Yin,[†,*] and Yuehe Lin[‡,*]

[†]School of Chemical Engineering and Technology, Harbin Institute of Technology, Harbin 150001, China, and [‡]Pacific Northwest National Laboratory, Richland, Washington 99352, United States. [§] These authors contributed equally to this work.

ABSTRACT Here we report that poly(diallyldimethylammonium chloride) (PDDA) acts as both a reducing agent and a stabilizer to prepare soluble graphene nanosheets from graphite oxide. The results of transmission electron microscopy, X-ray diffraction, X-ray photoelectron spectroscopy, atomic force microscopy, and Fourier transform infrared indicated that graphite oxide was successfully reduced to graphene nanosheets which exhibited single-layer structure and high dispersion in various solvents. The reaction mechanism for PDDA-induced reduction of exfoliated graphite oxide was proposed. Furthermore, PDDA facilitated the *in situ* growth of highly dispersed Pt nanoparticles on the surface of graphene nanosheets to form Pt/graphene nanocomposites, which exhibited excellent catalytic activity toward formic acid oxidation. This work presents a facile and environmentally friendly approach to the synthesis of graphene nanosheets and opens up a new possibility for preparing graphene and graphene-based nanomaterials for large-scale applications.

KEYWORDS: graphene · graphite oxide · PDDA · formic acid · Pt nanoparticles · electrocatalysts · *in situ* growth

Graphene, a one atom thick sheet of sp^2-bonded carbon, has attracted strong scientific and technological interest since its discovery in 2004.[1,2] Due to its huge surface area, excellent electric conductivity, and mechanical strength, graphene has shown great application potential in many fields, such as electronic devices,[3,4] energy storage and conversion,[5−7] and biosensors.[8−10] Micromechanical cleavage of layered graphite is the first procedure reported on preparing graphene. However, this method is not suitable for mass production.[1] Epitaxial growth *via* high-temperature treatment of silicon carbide[11,12] and chemical vapor deposition (CVD) of hydrocarbons on transition metal substrates such as nickel or copper[13] are two promising methods to provide the large-area and high-quality graphene wafers required for applications in electronics. Colloidal route, especially the one employing chemicals to reduce exfoliated graphite oxide (GO), is currently considered as one of the most attractive approaches.[14−17] The chemical reduction of GO is usually carried out using hydrazine or $NaBH_4$ as the reducing agents, which are highly toxic or explosive.[18,19] On the other hand, graphene nanosheets tend to form irreversible agglomerates through van der Waals attractive force, which leads to a great technical difficulty in the applications of graphene.[20,21] Recently, great efforts have been devoted to addressing this issue, among which attaching some molecules or polymers onto the surface of graphene nanosheets is a promising approach to obtain well-dispersed graphene suspension.[22,23] Therefore, an environmentally friendly approach to the large-scale production of soluble graphene is of great significance for its practical applications, which is still a great challenge.

Herein we report a scalable and eco-friendly method for preparation of soluble graphene. Poly(diallyldimethylammonium chloride) (PDDA), an ordinary polyelectrolyte, is able to adsorb on the surface of carbon nanotubes through $\pi-\pi$ interaction and electrostatic interaction,[24,25] which results in electrostatic repulsion between carbon nanotubes to prevent them from aggregating in water. Inspired by this, we employ PDDA to disperse graphene nanosheets; that is, positively charged PDDA first adsorbs onto the surface of GO (negatively charged) *via* the electrostatic interaction, and then during the reduction of GO, the adsorbed PDDA is expected to act as a stabilizer to make reduced GO (graphene) stable in water. Surprisingly, the addition of PDDA to GO aqueous solution induced an unexpected color change (from yellow-brown to black) as shown in Figure S1 in Supporting Information. Careful experiments revealed that exfoliated GO underwent a

* Address correspondence to yingphit@hit.edu.cn, yuehe.lin@pnl.gov.

Received for review September 20, 2010 and accepted February 21, 2011.

Published online March 01, 2011
10.1021/nn102467s

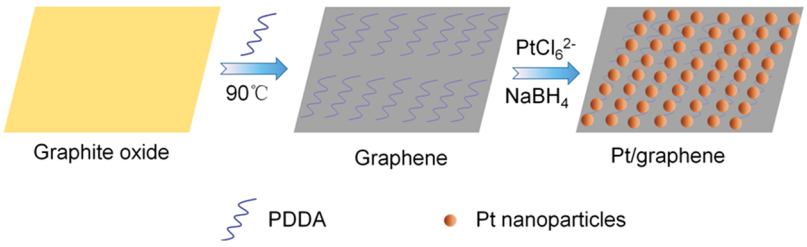

Scheme 1. Procedure for PDDA-induced reduction of graphite oxide and the *in situ* growth of Pt nanoparticles on them.

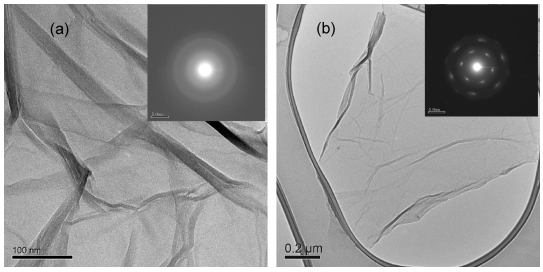

Figure 1. Typical TEM images and the corresponding SAED pattern of exfoliated graphite oxide (a) and graphene nanosheets (b).

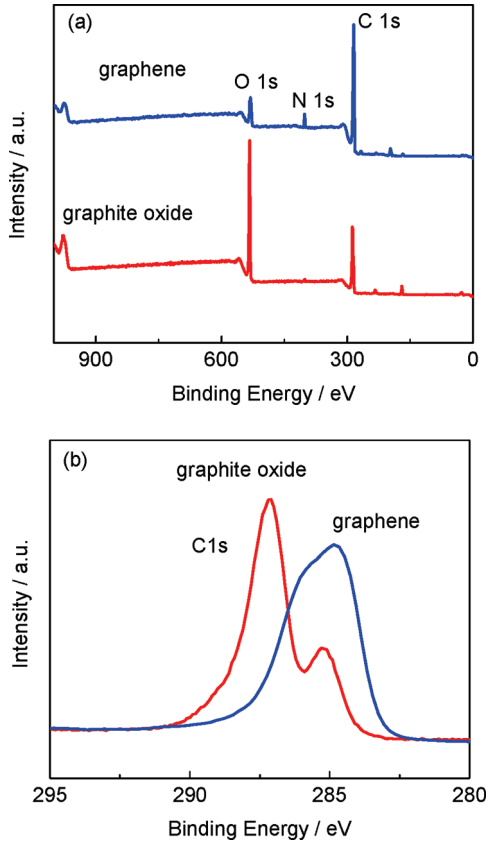

Figure 2. Survey XPS spectra (a) and C1s XPS spectra (b) of grahite oxide (GO) and graphene.

deoxygenation process in PDDA solution, and the obtained graphene nanosheets remained well-dispersed in water. To the best of our knowledge, this is the first time that polyelectrolyte is used as both a reducing agent and a stabilizer to prepare a colloidal suspension of graphene nanosheets. More importantly, the incorporation of PDDA as a "glue" molecule successfully turns graphene nanosheets into general platforms for *in situ* growth of Pt or Pd nanoparticles, which are demonstrated as promising electrocatalysts toward formic acid oxidation. The whole procedure for the synthesis of Pt/graphene is shown in Scheme 1.

TABLE 1. Relative Atomic Percentage of Various Functional Groups in GO and Reduced GO

		fitting of C1s (relative atomic percentage/%)				
	oxygen %	C—C	C—O/C—O—C	C—N	C=O	O—C=O
GO	56.6	24.5	58.4	0	14.2	3.0
graphene	15.5	52.7	33.8	4.5	7.0	2.0

RESULTS AND DISCUSSION

A facile synthesis of water-soluble graphene was developed. In brief, 60 mL of exfoliated GO suspension (0.5 mg mL^{-1}) in water and 600 μL of PDDA solution (35 wt % in water) were added into a three-necked flask. The temperature was controlled by a heating jacket, and the whole solution was subjected to vigorous stirring. The yellow-brown exfoliated GO suspension became black after it was kept at 90 °C for several hours. Figure 1a shows transmission electron microscopy (TEM) of exfoliated GO, which exhibits the typical wrinkle morphology.[5] The selected area electron diffraction (SAED) of GO further confirmed the disordered nature of GO.[26] When heated at 90 °C for 5 h, GO suspension changed from yellow-brown to black. TEM of the as-prepared material shown in Figure 1b exhibits a wrinkle-like thin sheet, which is the feature structure of graphene nanosheets. The corresponding SAED yields well-defined six-fold-symmetry diffraction patterns matching those expected for graphene nanosheets,[27−29] which indicates that GO is successfully reduced to graphene nanosheets.[30]

We employed X-ray photoelectron spectroscopy (XPS) to further confirm the reduction of GO. Figure 2a shows that the oxygen content in exfoliated GO

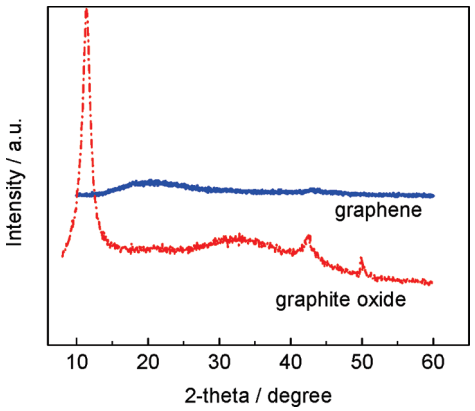

Figure 3. XRD patterns of graphite oxide (a) and graphene (b).

Figure 4. Digital photos of graphene (0.25 mg mL^{-1}) dispersed in different solvents: (left to right) H_2O, ethanol, glycol, and DMF.

decreased remarkably after the reduction, that is, 15.5% in graphene *versus* 56.6% in GO. Moreover, the oxygen content in the graphene prepared *via* conventional $NaBH_4$ reduction is 18.6% (Figure S2 in Supporting Information), which indicates a higher reduction degree in the PDDA-reduced graphene nanosheets. Figure 2b and Figure S3a,b in Supporting Information show the C1s peaks, which consist of five components arising from C−O−C/C−O (epoxyl and hydroxyl), C═O (carbonyl), O−C═O (carboxyl), and C−C.[31] The additional component at 285.9 eV in Figure S3a is assigned to the C−N bond.[32] The contents of the functional groups, which are calculated from areas of the contributing peaks, are listed in Table 1. The peak intensities of oxygen functionalities in graphene nanosheets are much smaller than that in GO. These observations indicate considerable deoxygenation through the PDDA reducing process. In addition, N1s spectra in Figure 2a and Figure S3c were observed in the graphene sample and suggested the presence of PDDA, which adsorbed on the surface of graphene nanosheets by $\pi-\pi$ and electrostatic interaction,[24] generating electrostatic repulsion between graphene nanosheets and resulting in a good dispersion in water (shown in Figure S1).

The obtained graphene is also characterized by the powder X-ray diffraction (XRD). As shown in Figure 3, the XRD pattern of GO exhibits a diffraction peak

Figure 5. Proposed reaction pathway for the deoxygenation of exfoliated GO in PDDA solution to obtain graphene nanosheets (G), where "R-N$^+$" was used to designate PDDA.

centered at 2θ = 11.4°, corresponding to the C(002) interlayer spacing of 0.78 nm,[5] which indicates the complete oxidation of graphite to GO.[22] This is a prerequisite for successfully exfoliating GO and obtaining graphene nanosheets.[33] After chemical reduction with PDDA, the diffraction peak of GO at 2θ = 11.4° disappears and a very broad peak around 20° is observed in the graphene sample, indicating that most oxygen functional groups were removed.[31] It should be noted that the diffraction peak in graphene nanosheets was rather broad and significantly different from that in graphite.[34]

The dispersion of graphene (0.25 mg mL^{-1}) in different solvents is shown in Figure 4. Homogeneous colloidal suspensions of graphene nanosheets are easily produced in H_2O, ethanol, glycol, and *N*,*N*-dimethylformamide (DMF), and these colloidal suspensions are stable for several months. Atomic force microscopy (AFM) image in Figure S4 shows that the average thickness of as-prepared graphene was about 1.1 nm, which is larger than the exfoliated GO sheets (less than 1 nm)[18] and normal single-sheet graphene (less than 0.9 nm).[14,21] It is reasonable to conclude that PDDA adsorbs on the surface of single-sheet graphene and increases the thickness of the obtained graphene. In addition, the ratio of the intensities of the {1100} to the {2110} can also give an unambiguous local identification of monolayer *versus* multilayer to provide information on the yield of monolayer graphene.[35] The relative intensity of the outer (I_{2110}) and inner (I_{1100}) circle spots in Figure 1b is measured to be <1, which indicates the single-layer structure of the resulting graphene nanosheets.[29,30,35]

To develop a more effective chemical reduction method to produce graphene nanosheets, it is necessary to elucidate the underlying reduction mechanism of GO. In the present study, it should be noted that, in the absence of PDDA, no color change was observed for the GO dispersion. This indicated that the formation of graphene can be attributed to the presence of PDDA, an ordinary polyelectrolyte with an ammonium group, which has been used as both a reducing and a stabilizing agent for preparing metal nanoparticles.[36,37] It has been reported that ammonium salts can be used as excellent catalysts for ring-opening reactions of epoxides.[38] Therefore, we propose a possible mechanism for deoxygenation of GO with PDDA (shown in Figure 5). Like hydrazine reducing GO, in step I, N^+ groups of PDDA attack the oxygen atom of epoxides in GO,[38,39]

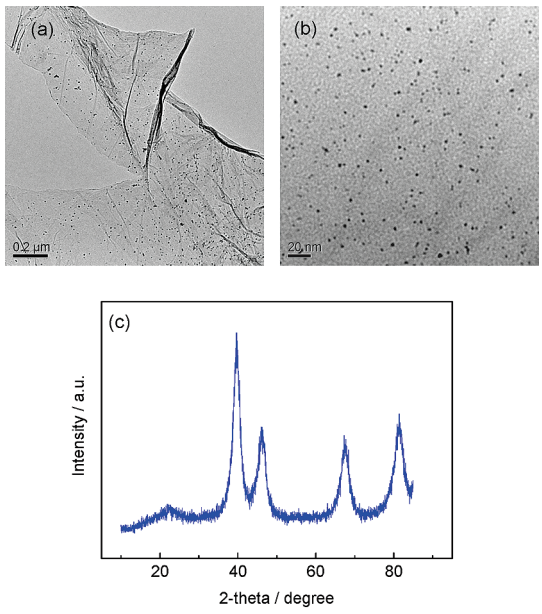

Figure 6. TEM images with different magnification (a,b) and XRD pattern of Pt/graphene.

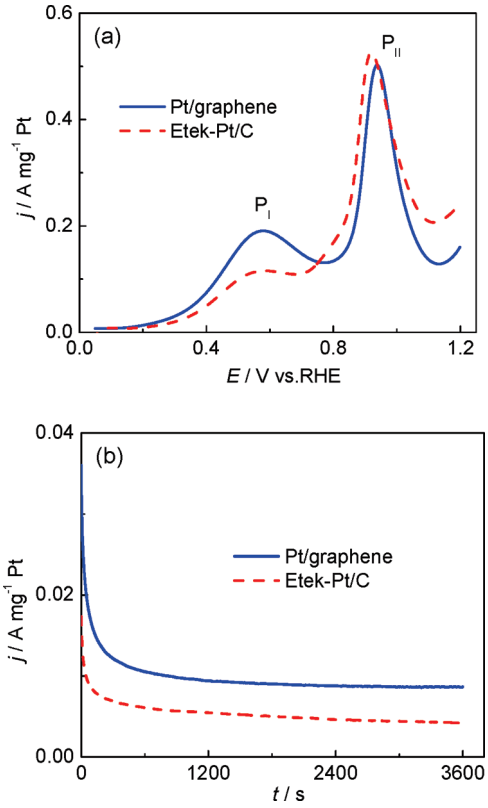

Figure 7. Formic acid oxidation (a) at the scan rate of 20 mV s^{-1} and amperometric *i*−*t* curves (b) at a fixed potential of 0.3 V on Pt/graphene and commercial Etek-Pt/C in N_2-saturated 0.5 M H_2SO4 + 0.5 M HCOOH.

which induces the ring-opening reaction (step II).[31,40] However, the ring opening of the epoxides with PDDA in itself would not result in any oxygen removal in GO. Previous study showed that, during the reduction of

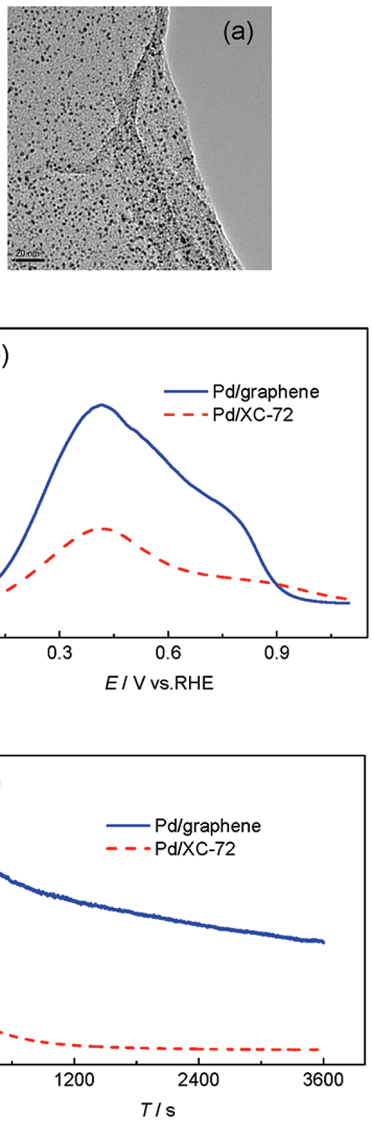

Figure 8. TEM image of Pd/graphene (a), formic acid oxidation (b) in N_2-saturated 0.5 M HCOOH and 0.5 M H_2SO_4, amperometric *i*−*t* curves (c) of HCOOH electro-oxidation at a fixed potential of 0.3 V on Pd/graphene and Pd/XC-72.

metal salts, the N^+ groups in PDDA were oxidized to the nitroso groups.[37] Fourier transform infrared (FTIR) spectroscopy of PDDA-reduced GO shows two peaks at 1385 and 831 cm^{-1} (Figure S5), which can be assigned to N−O and C−N vibrations, respectively.[37] This confirms that the nitroso groups are produced during the deoxygenation of GO. Therefore, it is reasonable that the initial derivative produced by the epoxide opening reacts further *via* the elimination of nitroso groups to form a C═C bond (shown in step III). This results in removing epoxides from GO, which is consistent with the XPS results above (the amount of C−O/C−O−C is significantly decreased). Most oxygen functionalities in GO are in the form of either hydroxyl or epoxide groups,[32] which has been confirmed by XPS. We have above proposed a possible mechanism for the re moval of epoxide groups by reducing GO with PDDA.

In contrast, the removal of a hydroxyl group (−OH) is considered as a thermal dehydroxylation process,[40,41] where the hydroxyl group directly leaves the graphene sheet with producing an OH radical and a graphene radical when GO suspension is heated.

Recently, graphene nanosheets with potentially low cost, high surface area, and good electrical conductivity, have been attracted considerable attentions as a promising candidate for fuel cell electrocatalyst supports.[42,43] However, only a few examples of Pt/graphene as fuel cell electrocatalysts have been demonstrated to date.[44−48] The possible reason is that it is difficult to uniformly load metal nanoparticles on graphene due to its hydrophobic property. In contrast, we find that the presence of PDDA on the surface of graphene facilitates the uniform distribution of Pt nanoparticles. PDDA adsorbed on the surface of graphene nanosheets acts as a glue molecule to facilitate the *in situ* growth of metal nanoparticles on the graphene surface. $PtCl_6^{2-}$ ions were first confined in the positively charged PDDA *via* electrostatic interaction and then reduced to Pt nanoparticles by $NaBH_4$. The presence of PDDA prevents Pt NPs from agglomeration. TEM images in Figure 6a,b show that Pt nanoparticles have a rather uniform dispersion on the surface of graphene nanosheets. The XRD pattern of Pt/graphene (Figure 6c) confirms that the average particle size of Pt is 3.0 nm calculated with Scherrer equation.[36]

The electrocatalytic activity toward formic acid oxidation on Pt/graphene was evaluated in the solution of 0.5 M H_2SO_4 + 0.5 M HCOOH. Generally, HCOOH oxidation on Pt usually follows the so-called dual pathway:[49]

I: Direct dehydrogenation producing CO_2.

$$HCOOH \rightarrow HCOO_{ads} + H^+ + e^-;\ HCOO_{ads} \rightarrow CO_2 + H^+ + e^-$$

II: Dehydration generating CO (poisoning intermediate).

$$HCOOH \rightarrow CO + H_2O \rightarrow CO_2 + 2H^+ + 2e^-$$

As displayed in Figure 7a, the P_I peak is related to the direct oxidation of HCOOH to CO_2, while the P_{II} peak is ascribed to the oxidation of the CO_{ads} generated from the dissociative adsorption step.[49] The P_I peak current densities on Pt/graphene are nearly two times that on commercial Etek-Pt/C, indicating much higher activity toward formic acid oxidation on Pt/graphene. In addition, the amperometric *i*−*t* curves (Figure 7b) also exhibit that Pt/graphene has a higher catalytic stability toward HCOOH oxidation.

Recently, Sutter *et al.* confirmed that the strong electronic interaction exists between graphene and metal NPs, which can affect adsorption energies of molecules on the metal NP surfaces.[50] Yoo *et al.* reported that the CO adsorption rate on Pt nano particles in Pt/graphene is much smaller than that in Pt/XC-72.[6] As shown in Figure 7a, the intensity of peak P_{II} on Pt/graphene is lower than that on Etek-Pt/C, thus indicating less CO formed on Pt/graphene during the oxidation of formic acid. Therefore, the reason for the high electrocatalytic activity of Pt/graphene is that the strong electronic interaction between Pt NPs and graphene suppresses the CO formation during the oxidation of formic acid, which facilitates the direct oxidation of HCOOH on the Pt surface.

Another important aspect is that this approach is not restricted to the synthesis of Pt/graphene alone. We also loaded Pd nanoparticles on graphene nanosheets (Pd/graphene) with the same method, where Pd nanoparticles were highly dispersed on graphene, as shown in Figure 8a. Compared with Pd/XC-72 catalyst, Pd/graphene exhibits significantly improved activity toward formic acid oxidation (Figure 8b). The *i*−*t* curves (Figure 8c) show that Pd/graphene has a higher catalytic stability toward HCOOH oxidation.[51]

To the best of our knowledge, this is the first report that polyelectrolyte is used as both a reducing agent and a stabilizer to prepare a colloidal suspension of graphene nanosheets. The advantages of this method are listed as follows. (1) Considering that PDDA is an eco-friendly chemical, this is a facile and environmentally friendly method for the preparation of the soluble graphene. (2) PDDA facilitates the uniform deposition of metal nanoparticles on graphene nanosheets. PDDA adsorbed on the surface of graphene nanosheets acts as a glue molecule to facilitate the *in situ* growth of metal nanoparticles on graphene surface. The obtained Pt/graphene with a high dispersion of Pt nanoparticles (~3.0 nm in diameter) exhibits much higher activity toward formic acid oxidation than Pt/XC-72. (3) A possible reaction mechanism for PDDA-induced reduction of exfoliated graphite oxide is proposed. N^+ groups of PDDA attack the oxygen atom of epoxides in GO, which induces the ring-opening reaction. The initial derivative produced by the epoxide opening reacts further *via* the elimination of nitroso groups to form a C=C bond. This results in oxygen removal from GO and formation of graphene.

CONCLUSIONS

In summary, we have developed a green and facile approach to prepare soluble graphene nanosheets. The key is the introduction of a positively charged polyelectrolyte, PDDA, which acts as both a reducing agent and a good stabilizer during the formation of graphene nanosheets. Another important role of PDDA is to facilitate the uniform deposition of metal nanoparticles on graphene nanosheets, which exhibit high activity toward formic acid oxidation. We therefore expect that our findings will lead to the further

development in preparation of high-quality graphene nanosheets and graphene-based nanocomposite, which may significantly facilitate the application of graphene in fuel cells and other fields.

EXPERIMENTAL SECTION

Synthesis of Graphene. The preparation procedure for graphite oxide (GO) is reported in our previous paper[5] and provided in Supporting Information. GO was deoxygenated using poly(diallyldimethylammonium chloride) (PDDA) as follows. Typically, a 60 mg GO powder in 20 mL of H_2O was sonicated for 10 min to form a homogeneous GO suspension, and 800 μL of 35 wt % PDDA solution was mixed with the GO suspension under vigorous stirring for 10 min. Then the solution was heated in refluxing conditions at 90 °C for 5 h. During this process, the color of the solution changed from yellow-brown to black. The resulting graphene suspension was filtered and washed with plenty of ultrapure water.

Synthesis of Pt/Graphene. Thirty milligrams of graphene nanosheets was redispersed in 200 mL of H_2O by sonication for 5 min. A 0.996 mL H_2PtCl_6 (7.53 mg of Pt per H_2O) solution was added dropwise under vigorous stirring for 10 min. Then 10 mg of $NaBH_4$ solved in 5 mL of H_2O was added dropwise to reduce H_2PtCl_6. After 48 h of stirring, the Pt/graphene suspension was filtered and then dried at 90 °C in vacuum for 3 h.

Physical Characterization. The TEM images of the catalysts were taken in a JEOL TEM 2010 microscope equipped with an Oxford ISIS system. The operating voltage on the microscope was 200 keV. All images were digitally recorded with a slow-scan CCD camera. X-ray diffraction (XRD) patterns were obtained using a Philips Xpert X-ray diffractometer using Cu Kα radiation at λ = 1.5418 Å. AFM images were recorded on a 5100 ALP (prototype Agilent Technologies) in tapping mode (dynamic force mode). Commercially available Si cantilevers with a force constant of 20 N/m were used as substrate. Fourier transform infrared (FTIR) analysis was carried out using a NICOLETiS10 spectrometer. The spectra were obtained by mixing the sample with KBr. The X-ray photoelectron spectroscopy (XPS) measurements were obtained on Physical Electronics Quantum 2000 scanning ESCA microprobe. This system uses a focused monochromatic aluminum K_ X-ray (1486.6 eV) source and a spherical section analyzer. The samples were dried in vacuum before the XPS test.

Electrochemical Measurements. The electrochemical tests were carried out in a standard three-electrode system controlled with a CHI660C station (CH Instruments, Inc., USA) with Pt wire and Hg/Hg_2SO_4 as the counter electrode and reference electrode, respectively. The working electrodes were prepared by applying catalyst ink onto the prepolished glass carbon disk electrodes. In brief, the electrocatalyst was dispersed in ethanol and ultrasonicated for 15 min to form a uniform catalyst ink (2 mg mL^{-1}). A total of 7.5 μL of well-dispersed catalyst ink was applied onto the prepolished glassy carbon (GC) disk electrode (5 mm in diameter). After drying at room temperature, a 2 $\times$ 5 μL 0.05 wt % Nafion solution was applied onto the surface of the catalyst layer to form a thin protective film. The total loading of the catalyst was 15 μg. The working electrodes were first activated with cyclic voltammograms (CVs) (0 to 1.1 V at 50 mV s^{-1}) in N_2-purged 0.5 M H_2SO_4 solution until a steady CV was obtained. To measure formic acid electro-oxidation, the solution of 0.5 M H_2SO_4 + 0.5 M HCOOH was purged with N_2 gas before measurements were taken, and the CV was recorded in the potential between 0.05 and 1.2 V at a scan rate of 50 mV s^{-1}. The amperometric current density−time (i−t) curves were measured at a fixed potential of 0.3 V for 1.5 h. All of the tests were conducted at room temperature. All potentials were reported *versus* the reversible hydrogen electrode (RHE).

Acknowledgment. The work was done at Pacific Northwest National Laboratory (PNNL) and was supported by a LDRD program. The characterization was performed using a national scientific-user facility sponsored by the DOE's Office of Biological and Environmental Research and located at PNNL. PNNL is operated for DOE by Battelle under Contract DE-AC05-76RL01830. We thank L. Wang for AFM and FTIR characterizations. S.Z. acknowledges a fellowship from the China Scholarship Council and PNNL to perform this work at PNNL. G.Y. acknowledges the support from National Science Foundation of China (No. 50872027).

Supporting Information Available: Synthesis of graphite oxide, AFM, FTIR, XRD, XPS, TEM images, and electrochemical measurements. This material is available free of charge *via* the Internet at http://pubs.acs.org.

REFERENCES AND NOTES

1. Novoselov, K. S.; Geim, A. K.; Morozov, S. V.; Jiang, D.; Zhang, Y.; Dubonos, S. V.; Grigorieva, I. V.; Firsov, A. A. Electric Field Effect in Atomically Thin Carbon Films. *Science* **2004,** *306*, 666–669.
2. Rao, C. N. R.; Sood, A. K.; Subrahmanyam, K. S.; Govindaraj, A. Graphene: The New Two-Dimensional Nanomaterial. *Angew. Chem., Int. Ed.* **2009,** *48*, 7752–7777.
3. Dikin, D. A.; Stankovich, S.; Zimney, E. J.; Piner, R. D.; Dommett, G. H. B.; Evmenenko, G.; Nguyen, S. T.; Ruoff, R. S. Preparation and Characterization of Graphene Oxide Paper. *Nature* **2007,** *448*, 457–460.
4. Meng, X. B.; Geng, D. S.; Liu, J. A.; Banis, M. N.; Zhang, Y.; Li, R. Y.; Sun, X. L. Non-aqueous Approach To Synthesize Amorphous/Crystalline Metal Oxide-Graphene Nanosheet Hybrid Composites. *J. Phys. Chem. C* **2010,** *114*, 18330–18337.
5. Shao, Y. Y.; Wang, J.; Engelhard, M.; Wang, C. M.; Lin, Y. H. Facile and Controllable Electrochemical Reduction of Graphene Oxide and Its Applications. *J. Mater. Chem.* **2010,** *20*, 743–748.
6. Yoo, E.; Okata, T.; Akita, T.; Kohyama, M.; Nakamura, J.; Honma, I. Enhanced Electrocatalytic Activity of Pt Subnanoclusters on Graphene Nanosheet Surface. *Nano Lett.* **2009,** *9*, 2255–2259.
7. Qu, L. T.; Liu, Y.; Baek, J. B.; Dai, L. M. Nitrogen-Doped Graphene as Efficient Metal-Free Electrocatalyst for Oxygen Reduction in Fuel Cells. *ACS Nano* **2010,** *4*, 1321–1326.
8. Tang, L. H.; Wang, Y.; Li, Y. M.; Feng, H. B.; Lu, J.; Li, J. H. Preparation, Structure, and Electrochemical Properties of Reduced Graphene Sheet Films. *Adv. Funct. Mater.* **2009,** *19*, 2782–2789.
9. Shao, Y. Y.; Zhang, S.; Engelhard, M. H.; Li, G. S.; Shao, G. C.; Wang, Y.; Liu, J.; Aksay, I. A.; Lin, Y. H. Nitrogen-Doped Graphene and Its Electrochemical Applications. *J. Mater. Chem.* **2010,** *20*, 7491–7496.
10. Wang, Y.; Shao, Y. Y.; Matson, D. W.; Li, J. H.; Lin, Y. H. Nitrogen-Doped Graphene and Its Application in Electrochemical Biosensing. *ACS Nano* **2010,** *4*, 1790–1798.
11. Berger, C.; Song, Z. M.; Li, X. B.; Wu, X. S.; Brown, N.; Naud, C.; Mayou, D.; Li, T. B.; Hass, J.; Marchenkov, A. N. *et al.* Electronic Confinement and Coherence in Patterned Epitaxial Graphene. *Science* **2006,** *312*, 1191–1196.
12. Emtsev, K. V.; Bostwick, A.; Horn, K.; Jobst, J.; Kellogg, G. L.; Ley, L.; McChesney, J. L.; Ohta, T.; Reshanov, S. A.; Rohrl, J.; *et al.*Towards Wafer-Size Graphene Layers by Atmospheric Pressure Graphitization of Silicon Carbide. *Nat. Mater.* **2009,** *8*, 203–207.
13. Kim, K. S.; Zhao, Y.; Jang, H.; Lee, S. Y.; Kim, J. M.; Ahn, J. H.; Kim, P.; Choi, J. Y.; Hong, B. H. Large-Scale Pattern Growth of Graphene Films for Stretchable Transparent Electrodes. *Nature* **2009,** *457*, 706–710.
14. Fan, X. B.; Peng, W. C.; Li, Y.; Li, X. Y.; Wang, S. L.; Zhang, G. L.; Zhang, F. B. Deoxygenation of Exfoliated Graphite Oxide

under Alkaline Conditions: A Green Route to Graphene Preparation. *Adv. Mater.* **2008,** *20*, 4490–4493.
15. Li, X. L.; Wang, X. R.; Zhang, L.; Lee, S. W.; Dai, H. J. Chemically Derived, Ultrasmooth Graphene Nanoribbon Semiconductors. *Science* **2008,** *319*, 1229–1232.
16. Wang, L.; Tian, C. G.; Wang, H.; Ma, Y. G.; Wang, B. L.; Fu, H. G. Mass Production of Graphene *via* an *In-Situ* Self-Generating Template Route and Its Promoted Activity as Electrocatalytic Support for Methanol Electroxidization. *J. Phys. Chem. C* **2010,** *114*, 8727–8733.
17. Zhang, J. L.; Yang, H. J.; Shen, G. X.; Cheng, P.; Zhang, J. Y.; Guo, S. W. Reduction of Graphene Oxide *via* L-Ascorbic Acid. *Chem. Commun.* **2010,** *46*, 1112–1114.
18. Zhu, C. Z.; Guo, S. J.; Fang, Y. X.; Dong, S. J. Reducing Sugar: New Functional Molecules for the Green Synthesis of Graphene Nanosheets. *ACS Nano* **2010,** *4*, 2429–2437.
19. Liu, J. B.; Fu, S. H.; Yuan, B.; Li, Y. L.; Deng, Z. X. Toward a Universal "Adhesive Nanosheet" for the Assembly of Multiple Nanoparticles Based on a Protein-Induced Reduction/Decoration of Graphene Oxide. *J. Am. Chem. Soc.* **2010,** *132*, 7279–7281.
20. Liang, Y. Y.; Wu, D. Q.; Feng, X. L.; Mullen, K. Dispersion of Graphene Sheets in Organic Solvent Supported by Ionic Interactions. *Adv. Mater.* **2009,** *21*, 1679–1683.
21. Li, D.; Muller, M. B.; Gilje, S.; Kaner, R. B.; Wallace, G. G. Processable Aqueous Dispersions of Graphene Nanosheets. *Nat. Nanotechnol.* **2008,** *3*, 101–105.
22. Xu, Y. X.; Bai, H.; Lu, G. W.; Li, C.; Shi, G. Q. Flexible Graphene Films *via* the Filtration of Water-Soluble Noncovalent Functionalized Graphene Sheets. *J. Am. Chem. Soc.* **2008,** *130*, 5856–5857.
23. Ramanathan, T.; Abdala, A. A.; Stankovich, S.; Dikin, D. A.; Herrera-Alonso, M.; Piner, R. D.; Adamson, D. H.; Schniepp, H. C.; Chen, X.; Ruoff, R. S.; Nguyen, S. T.;*et al.*Functionalized Graphene Sheets for Polymer Nanocomposites. *Nat. Nanotechnol.* **2008,** *3*, 327–331.
24. Yang, D. Q.; Rochette, J. F.; Sacher, E. Spectroscopic Evidence for $\pi-\pi$ Interaction between Poly(diallyl dimethylammonium) Chloride and Multiwalled Carbon Nanotubes. *J. Phys. Chem. B* **2005,** *109*, 4481–4484.
25. Zhang, S.; Shao, Y. Y.; Yi, G. P.; Lin, Y. H. Self-Assembly of Pt Nanoparticles on Highly Graphitized Carbon Nanotubes as an Excellent Oxygen-Reduction Catalyst. *Appl. Catal. B* **2011,** *102*, 372–377.
26. Wang, G. X.; Yang, J.; Park, J.; Gou, X. L.; Wang, B.; Liu, H.; Yao, J. Facile Synthesis and Characterization of Graphene Nanosheets. *J. Phys. Chem. C* **2008,** *112*, 8192–8195.
27. Chen, Y.; Zhang, X.; Yu, P.; Ma, Y. W. Stable Dispersions of Graphene and Highly Conducting Graphene Films: A New Approach to Creating Colloids of Graphene Monolayers. *Chem. Commun.* **2009,** 4527–4529.
28. Meyer, J. C.; Geim, A. K.; Katsnelson, M. I.; Novoselov, K. S.; Booth, T. J.; Roth, S. The Structure of Suspended Graphene Sheets. *Nature* **2007,** *446*, 60–63.
29. Gao, W.; Alemany, L. B.; Ci, L. J.; Ajayan, P. M. New Insights into the Structure and Reduction of Graphite Oxide. *Nat. Chem.* **2009,** *1*, 403–408.
30. Zhang, W. X.; Cui, J. C.; Tao, C. A.; Wu, Y. G.; Li, Z. P.; Ma, L.; Wen, Y. Q.; Li, G. T. A Strategy for Producing Pure Single-Layer Graphene Sheets Based on a Confined Self-Assembly Approach. *Angew. Chem., Int. Ed.* **2009,** *48*, 5864–5868.
31. Shin, H. J.; Kim, K. K.; Benayad, A.; Yoon, S. M.; Park, H. K.; Jung, I. S.; Jin, M. H.; Jeong, H. K.; Kim, J. M.; Choi, J. Y.;*et al.* Efficient Reduction of Graphite Oxide by Sodium Borohydrilde and Its Effect on Electrical Conductance. *Adv. Funct. Mater.* **2009,** *19*, 1987–1992.
32. Stankovich, S.; Dikin, D. A.; Piner, R. D.; Kohlhaas, K. A.; Kleinhammes, A.; Jia, Y.; Wu, Y.; Nguyen, S. T.; Ruoff, R. S. Synthesis of Graphene-Based Nanosheets *via* Chemical Reduction of Exfoliated Graphite Oxide. *Carbon* **2007,** *45*, 1558–1565.
33. McAllister, M. J.; Li, J. L.; Adamson, D. H.; Schniepp, H. C.; Abdala, A. A.; Liu, J.; Herrera-Alonso, M.; Milius, D. L.; Car, R.; Prud'homme, R. K.;*et al.*A. Single Sheet Functionalized Graphene by Oxidation and Thermal Expansion of Graphite. *Chem. Mater.* **2007,** *19*, 4396–4404.
34. Zhang, S.; Shao, Y. Y.; Li, X. H.; Nie, Z. M.; Wang, Y.; Liu, J.; Yin, G. P.; Lin, Y. H. Low-Cost and Durable Catalyst Support for Fuel Cells: Graphite Submicronparticles. *J. Power Sources* **2010,** *195*, 457–460.
35. Hernandez, Y.; Nicolosi, V.; Lotya, M.; Blighe, F. M.; Sun, Z. Y.; De, S.; McGovern, I. T.; Holland, B.; Byrne, M.; Gun'ko, Y. K.;*et al.*High-Yield Production of Graphene by Liquid-Phase Exfoliation of Graphite. *Nat. Nanotechnol.* **2008,** *3*, 563–568.
36. Zhang, S.; Shao, Y. Y.; Yin, G. P.; Lin, Y. H. Stabilization of Platinum Nanoparticle Electrocatalysts for Oxygen Reduction Using Poly(diallyldimethylammonium chloride). *J. Mater. Chem.* **2009,** *19*, 7995–8001.
37. Chen, H.; Wang, Y.; Dong, S. An Effective Hydrothermal Route for the Synthesis of Multiple PDDA-Protected Noble-Metal Nanostructures. *Inorg. Chem.* **2007,** *46*, 10587–10593.
38. Fogassy, G.; Pinel, C.; Gelbard, G. Solvent-Free Ring Opening Reaction of Epoxides Using Quaternary Ammonium Salts as Catalyst. *Catal. Commun.* **2009,** *10*, 557–560.
39. Mahesh, M.; Murphy, J. A.; Wessel, H. P. Novel Deoxygenation Reaction of Epoxides by Indium. *J. Org. Chem.* **2005,** *70*, 4118–4123.
40. Gao, X. F.; Jang, J.; Nagase, S. Hydrazine and Thermal Reduction of Graphene Oxide: Reaction Mechanisms, Product Structures, and Reaction Design. *J. Phys. Chem. C* **2010,** *114*, 832–842.
41. Xu, S. C.; Irle, S.; Musaev, D. G.; Lin, M. C. Quantum Chemical Study of the Dissociative Adsorption of OH and H_2O on Pristine and Defective Graphite (0001) Surfaces: Reaction Mechanisms and Kinetics. *J. Phys. Chem. C* **2007,** *111*, 1355–1365.
42. Zhang, S.; Shao, Y. Y.; Liao, H. G.; Liu, J.; Aksay, I. A.; Yin, G. P.; Lin, Y. H. Graphene Decorated with PtAu Alloy Nanoparticles: Facile Synthesis and Promising Application for Formic Acid Oxidation. *Chem. Mater.* **2011,** *23*, 1079–1081.
43. Xu, C.; Wang, X.; Zhu, J. W. Graphene−Metal Particle Nanocomposites. *J. Phys. Chem. C* **2008,** *112*, 19841–19845.
44. Shao, Y. Y.; Zhang, S.; Wang, C. M.; Nie, Z. M.; Liu, J.; Wang, Y.; Lin, Y. H. Highly Durable Graphene Nanoplatelets Supported Pt Nanocatalysts for Oxygen Reduction. *J. Power Sources* **2010,** *195*, 4600–4605.
45. Kou, R.; Shao, Y. Y.; Wang, D. H.; Engelhard, M. H.; Kwak, J. H.; Wang, J.; Viswanathan, V. V.; Wang, C. M.; Lin, Y. H.; Wang, Y..;*et al.*Enhanced Activity and Stability of Pt Catalysts on Functionalized Graphene Sheets for Electrocatalytic Oxygen Reduction. *Electrochem. Commun.* **2009,** *11*, 954–957.
46. Guo, S. J.; Dong, S. J.; Wang, E. K. Three-Dimensional Pt-on-Pd Bimetallic Nanodendrites Supported on Graphene Nanosheet: Facile Synthesis and Used as an Advanced Nanoelectrocatalyst for Methanol Oxidation. *ACS Nano* **2010,** *4*, 547–555.
47. Seger, B.; Kamat, P. V. Electrocatalytically Active Graphene−Platinum Nanocomposites. Role of 2-D Carbon Support in PEM Fuel Cells. *J. Phys. Chem. C* **2009,** *113*, 7990–7995.
48. Li, Y. M.; Tang, L. H.; Li, J. H. Preparation and Electrochemical Performance for Methanol Oxidation of Pt/Graphene Nanocomposites. *Electrochem. Commun.* **2009,** *11*, 846–849.
49. Zhang, S.; Shao, Y. Y.; Yin, G. P.; Lin, Y. H. Electrostatic Self-Assembly of Pt-around-Au Nanocomposite with High Activity towards Formic Acid Oxidation. *Angew. Chem., Int. Ed.* **2010,** *49*, 2211–2214.
50. Sutter, P.; Sadowski, J. T.; Sutter, E. A. Chemistry under Cover: Tuning Metal−Graphene Interaction by Reactive Intercalation. *J. Am. Chem. Soc.* **2010,** *132*, 8175–8179.
51. Wang, J. J.; Chen, Y. G.; Liu, H.; Li, R. Y.; Sun, X. L. Synthesis of Pd Nanowire Networks by a Simple Template-Free and Surfactant-Free Method and Their Application in Formic Acid Electrooxidation. *Electrochem. Commun.* **2010,** *12*, 219–222.